Base-Pairing Properties of 8-Aza-7-deazaadenine Linked *via* the 8-Position to the DNA Backbone

by **Frank Seela***, **Matthias Zulauf**, and **Harald Debelak**

Laboratorium für Organische und Bioorganische Chemie, Institut für Chemie, Universität Osnabrück, Barbarastr. 7, D-49069 Osnabrück, Germany (fax: +49(541)969-2370; email: Fraseela@rz.uni-osnabrueck.de)

The base-pairing properties of oligonucleotides containing the unusual N^8-linked 8-aza-7-deazaadenine 2′-deoxyribonucleoside (**2a**) as well as its 7-bromo derivative **2b** are described. The oligonucleotides were prepared by solid-phase synthesis employing phosphoramidite chemistry. Compound **2a** forms a strong base pair with T_d for which a reverse *Watson-Crick* pair is suggested (*Fig. 9*). Compound **2a** displays a lower *N*-glycosylic-bond stability than its N^9-nucleoside and shows strong stacking interactions when incorporated into oligonucleotides. The replacement of 2′-deoxyadenosine by **2a** does not significantly influence the duplex stability. However, this behavior depends on the position of the incorporation.

Introduction. – The current knowledge of usual DNA structures such as hairpins, cruciforms, triplexes, tetraplexes, or pentaplexes or left-handed Z-DNA is related to special sequence motifs [1]. Also, changes in the environmental conditions, such as counter ions, or the interaction with high-molecular-weight proteins that bind to DNA can alter the nucleic acid structure [2]. The variety of DNA structures is increased by those of backbone-modified nucleic acids (PNA, hexose-DNA, bicyclo-DNA) or DNA containing modified nucleobases (7-deazapurines, isoguanine) [3–7].

Earlier, it was shown that purine N^7-(2′-deoxyribofuranosides) related to 2′-deoxyadenosine or 2′-deoxyguanosine form stable base pairs in duplex DNA [8][9]. It was also found that the N^8-glycosylated 8-azaadenine (pyrazolo[3,4-*d*]pyrimidin-4-amine; purine numbering is used throughout the *General Part*) forms a rather stable base pair with thymidine when it replaces 2′-deoxyadenosine in self-complementary duplexes such as 5′-d(A-T)$_6$-3′ or 5′-d(C-T-G-G-A-T-C-C-A-G)-3′ [10]. As this

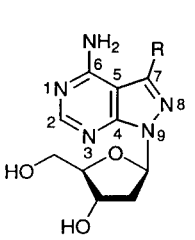

1a R = H
b R = Br
c R = I

Purine numbering

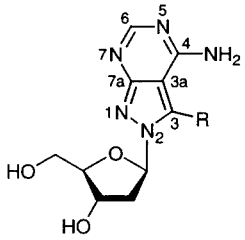

2a R = H
b R = Br
c R = I

Systematic numbering

observation was unexpected, we decided to investigate this subject in more detail. For this purpose, we incorporated the N^8-linked nucleoside **2a** [10][11] into a series of self-complementary and non-self-complementary oligonucleotides and studied their base-pairing properties. Furthermore, the influence of bulky substituents at the 7-position (see **2b**) were examined. For comparison, hybridization experiments were performed with oligonucleotides containing the regular (N^9-linked) 8-aza-7-deazaadenine 2′-deoxyribonucleoside (**1a**) [10][11].

Results and Discussion. – 1. *Monomers.* The glycosylation of 8-aza-7-deaza-6-methoxypurine (**3a**) as well as of the 7-bromo or 7-iodo derivatives **3b**,**c** with 2′-deoxyribofuranosyl chloride **4** gave the N^9-nucleosides **6a**–**c** as main products, while the N^8-compounds **5a**–**c** were formed as the minor components [11–13]. The regularly linked nucleosides **1a**–**c** were prepared as described earlier [11][13]. Detoluoylation of the intermediates **5b**,**c** (methanolic ammonia) furnished the deprotected nucleosides **2b**,**c** under simultaneous displacement of the MeO group by the NH_2 function (*Scheme 1*). The halogen substituents could be retained under these conditions, and a cleavage of the *N*-glycosylic bond was not observed. The chromatographic mobility of

Scheme 1

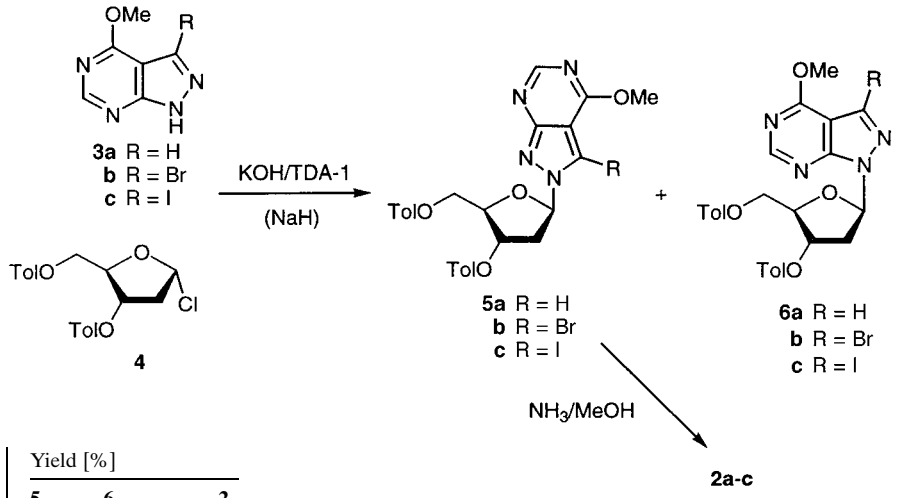

	Yield [%]		
	5	**6**	**2**
a	25	56	89
b	8 (15)	44 (34) [13]	44
c	11 (18)	38 (38) [13]	48

the N^8-glycosylated compounds **2a**–**c** (HPLC (*RP-18*); *Fig. 1*) points to a higher polarity of the N^8-nucleosides compared to their N^9-counterparts **1a**–**c**. As the corresponding adenine N^7-(2′-deoxyribonucleosides) *vs.* their N^9-isomers do not show such behavior [9], the presence of the *o*-quinoid moiety in **2a**–**c** might be responsible for the increased polarity. The 7-iodo derivative **1c** served as starting material for the

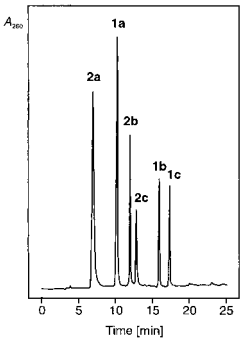

Fig. 1. *HPLC Profiles of the 8-aza-7-deazaadenine* N^9*-deoxyribonucleosides* **1a**–**c** *and of their* N^8*-regioisomers* **2a**–**c**

Table 1. *Half-life Values* (τ) *of Proton-Catalyzed Glycosylic-Bond Hydrolysis of the* N^8*-Linked 8-Aza-7-deazaadenine 2′-Deoxyribonucleosides* **2a**–**c** *and of Their* N^9*-Derivates* **1a**–**c**

	τ [min][a])	λ [nm]
$N^8c^7z^8A_d$ (**2a**) [15]	16	268, 280
$N^8Br^7c^7z^8A_d$ (**2b**)	< 1 (13)[b])	271, 293
$N^8I^7c^7z^8A_d$ (**2c**)	3 (51)[b])	275, 300
$c^7z^8A_d$ (**1a**) [15]	61	258
$I^7c^7z^8A_d$ (**1c**)	300	233
A_d [15]	3.5	

[a]) Measured UV-spectrophotometrically in 1.0N HCl at 25°. [b]) Measured UV-spectrophotometrically in 0.1N HCl.

palladium(0)-catalyzed cross-coupling reaction with hex-1-yne [12]. Although the 7-alkynylated N^9-nucleosides were obtained under those conditions [12], the coupling reaction failed in the case of the N^8-linked iodo isomer **2c**. Instead, the deiodinated N^8-nucleoside **2a** was obtained as established by NMR spectroscopy.

Next, the glycosylic-bond stability of **2a**–**c** was investigated in acidic medium. The reaction was followed UV-spectrophotometrically in 1.0M and 0.1M HCl at 25°. The acid stability of the regularly linked nucleoside **1a** is significantly higher than that of the N^8-nucleoside **2a** or 2′-deoxyadenosine [11][12] (*Table 1*). Similarly, the N^8-nucleosides **2b**,**c** carrying a halogen atom at C(7) are more labile than the regularly linked nucleosides **1b**,**c** while the *N*-glycosylic bond of the latter is stabilized by the halogen substituent at C(7). The behavior of the halogenated N^8-nucleosides is similar to that of the 8-halogenated purine N^9-nucleosides, which are always less stable than their non-halogenated counterparts [14].

It is expected that the nucleosides **2a**–**c** show a dynamic conformational equilibrium in solution as it is found for the canonical DNA constituents. The conformational states are described by *i*) the puckering of the pentofuranosyl moiety ($N \leftrightarrow S$, ${}^{3'}T_{2'} \leftrightarrow {}_{3'}T^{2'}$), *ii*) the rotational equilibrium about the C(4′)–C(5′) bond ($\gamma^{g+} \leftrightarrow \gamma^{t} \leftrightarrow \gamma^{g-}$), as well as by *iii*) the *syn-anti* equilibrium of the base around the *N*-glycosylic bond [16]. The nucleobases linked to the anomeric sugar C-atom drive the two-state ($N \leftrightarrow S$) pseudorotational equilibrium in nucleosides by two counteracting contributions [17]: *i*) the anomeric effect (stereoelectronic interactions between O(4′) and the nucleobase N-atom at C(1′)), which places the aglycone in the pseudoaxial orientation and *ii*) the inherent steric effect of the nucleobase, which opposes the anomeric effect by its tendency to take up the pseudoequatorial position (*Fig. 2*). The latter is sterically favored in the *S*-type conformation.

The sugar conformation of the nucleosides **1a**–**c** and **2a**–**c** was determined from the vicinal ^3J(H,H) coupling constants of the ^{1}H-NMR spectra measured in D_2O (*Table 2*) by the PSEUROT program [18][19]. In the case of 2′-deoxyadenosine, the preferred conformation is *S* (72%, *Table 3*) [20]. This *S*-conformer population is decreased in the case of the pyrazolo[3,4-*d*]pyrimidine nucleosides **1a**–**c**. A further

North (*N*) β-D-sugar (C(3')-*endo*-C(2')-*exo*) ⇌ South (*S*) β-D-sugar (C(2')-*endo*-C(3')-*exo*)

Fig. 2. *Two-state* ($N \leftrightarrow S$) *pseudorotational equilibrium of a 2′-deoxynucleoside*

Table 2. ^{3}J *Coupling Constants* [Hz] *of the Sugar Protons of the* N^8*-Linked 8-Aza-7-deazaadenine 2′-Deoxyribonucleosides* **2a**–**c** *and for Comparison of Their* N^9*-Isomers* **1a**–**c**

	$^3J(1',2')$	$^3J(1',2'')$	$^3J(2',3')$	$^3J(2'',3')$	$^3J(3',4')$	$^3J(4',5')$	$^3J(4',5'')$
A_d[a])	7.2	6.5	6.5	3.3	3.3	3.5	4.3
1a[a])	6.6	6.7	6.5	4.0	3.7	4.0	5.9
b[a])	6.4	6.4	6.6	4.5	3.3	4.4	6.0
c[a])	6.3	6.5	6.6	4.1	3.4	4.8	6.0
2a[a])	6.0	6.4	6.0	4.6	4.1	3.8	5.9
b[b])	5.0	6.9	6.4	4.9	4.4	4.1	6.3
c[b])	5.9	6.6	5.7	5.0	4.4	4.1	6.1
z^8A_d [21][a])	6.5	6.6	5.7	5.2	5.2	3.7	5.8
$N^8z^8A_d$ [21][a])	4.1	6.8	6.5	6.6	4.3	3.9	6.5

[a]) Measured in D_2O at 20°. [b]) Measured in D_2O/(D_6)DMSO 95 : 5 at 35°.

decrease occurs in the case of the N^8-nucleosides **2a**–**c**, which show an almost equal population of *S*- and *N*-conformers. This trend proceeds when the conformer population of 8-aza-2′-deoxyadenosine (*Table 3*) is examined. This behavior indicates that nucleobases with electron-attracting properties drive the equilibrium from *S*-towards the *N*-conformation. Concerning the conformation about the C(4′)–C(5′) bond, the following relationship is observed: ($\gamma^{g+} \leftrightarrow \gamma^{t} \leftrightarrow \gamma^{g-}$) (*Fig. 3*, *Table 3*). While

Table 3. *Calculated Pseudorotational Parameters and the Rotational Equilibrium about the C(4′)–C(5′) Bond of the 8-Aza-7-deazaadenine 2′-deoxyribonucleosides* **1a**–**c** *and* **2a**–**c**[a])

	%*N*	%*S*	% $\gamma^{g+}(+sc)$	% $\gamma^{t}(-sc)$	% γ^{g-} (*ap*)
A_d	28	72	59	25	16
1a	37	63	35	43	22
b	39	61	29	44	25
c	37	63	25	44	31
2a	44	56	38	42	20
b	48	52	29	48	23
c	47	53	31	46	23
z^8A_d [22]	50	50	39	42	19
$N^8z^8A_d$ [22]	59	41	29	50	21

[a]) R.m.s. ≤ 0.4 for all calculations; $|\Delta J_{max}| \leq 0.5$ Hz.

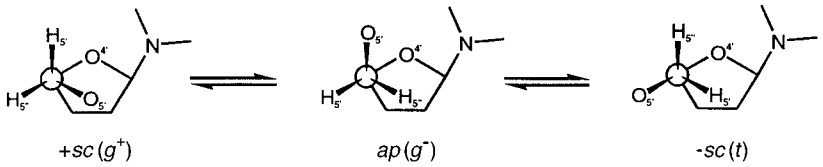

Fig. 3. *Conformations about the C(4′)–C(5′) bond of* **1a–c** *and* **2a–c**

A_d shows a $+sc$ rotamer population of 59%, it decreases to 38% for the N^8-glycosylated nucleoside **2a**. This phenomenon is similar to that found for the related pyrazolo[3,4-*d*]pyrimidine and triazolo[4,5-*d*]pyrimidine nucleosides but opposite to that of 7-substituted 7-deazapurine nucleosides [21][22].

Single-crystal X-ray analyses show that the regularly linked pyrazolo[3,4-*d*]-pyrimidine nucleosides of type **1** show a rather different *N*-glycosylic-bond conformation (*high-anti*) compared to the purine nucleosides [23]; these changes are also observed in the CD spectra [23]. *Fig. 4,a*, shows that a change of the glycosylation position from N^9 to N^8 as in **1a–c** *vs.* **2a–c** reverses the sign of the *Cotton* effect in the CD spectra and shifts the signal to longer wavelength. According to *Fig. 4,b*, the UV maximum of **1a** (*ca.* 280 nm) is shifted to a longer wavelength compared to that of 2′-deoxyadenosine (260 nm); in **2a**,**b** the quinoid structure gives rise to a further shift of the UV-maximum.

The phosphoramidites **9** and **10** were synthesized as the starting materials for the oligonucleotide synthesis. Compound **9** was prepared as described earlier [10]. The (dimethylamino)ethylidene residue was chosen as amino protecting group of the 7-brominated nucleoside ($\rightarrow$**7**). The half-life value of the deprotection of compound **7** which was determined UV-spectrophotometrically in 25% aqueous NH_3 solution was 36 min at 20°. Subsequently, the 4,4′-dimethoxytriphenylmethyl group was introduced furnishing the derivative **8** (*Scheme 2*). Phosphitylation of compound **8** with 2-cyanoethyl diisopropylphosphoramidochloridite furnished the phosphoramidite **10** (63% yield).

All compounds were characterized by ^{1}H-, ^{13}C-, and ^{31}P-NMR spectroscopy (for ^{13}C-NMR, see *Table 4*; for ^{1}H-NMR, see *Exper. Part*) as well as by elemental analyses or FAB-MS. The ^{13}C-NMR signals of the 8-aza-7-deaza-2′-deoxyadenosine derivatives **2b**,**c**, **7**, and **8** were assigned by gated-decoupled ^{13}C-NMR or heteronuclear ^{1}H/^{13}C-NMR correlation spetra. The ^{13}C-NMR data indicate a significant upfield shift of the C(7) signal when the glycosylic position is changed from N(9) to N(8). The introduction of the acetamidine protecting group ($\rightarrow$**7**) has a strong impact on the ^{13}C-NMR chemical shifts of the heterocyclic system.

2. *Oligonucleotides.* 2.1. *Synthesis.* To investigate the base-pairing properties of the N^8-nucleosides **2a**,**b**, a series of oligonucleotides was synthesized. Automated solid-phase synthesis was performed with the methyl phosphoramidite **9** [10] or the corresponding cyanoethyl phosphoramidite, described elsewhere [24], as well as the cyanoethyl phosphoramidite **10**. The coupling yields were always higher than 95%. Deprotection was performed with 25% aqueous NH_3 solution and purification by OPC cartridges [26] or by reversed-phase HPLC (see *Exper. Part*). The oligonucleotides that were synthesized with the methyl phosphoramidite were demethylated with thiophe-

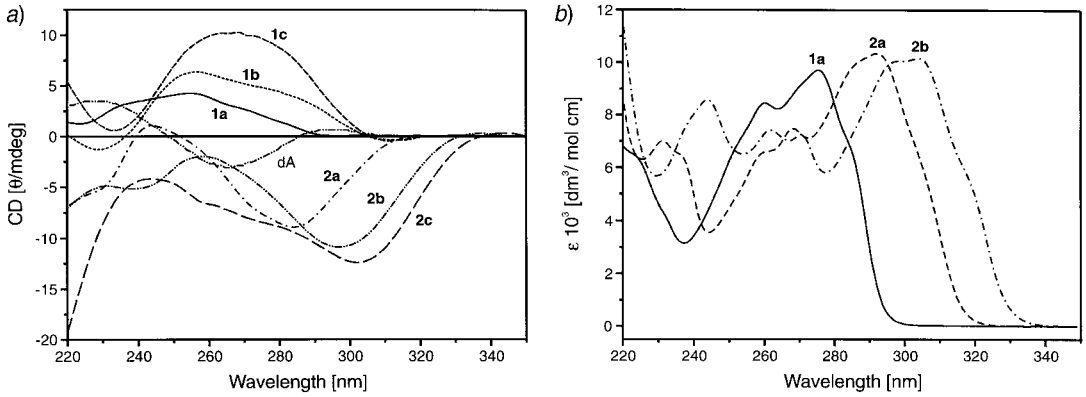

Fig. 4. a) *CD Spectra of the nucleosides* **1b**,**c** and **2b**,**c**; b) *UV spectra of the* N^9*-nucleoside* **1a**, *the* N^8*-nucleoside* **2a**, *and its 7-bromo derivative* **2b**. Measured at 10° in bidistilled water with 10 mM nucleoside concentration.

Scheme 2

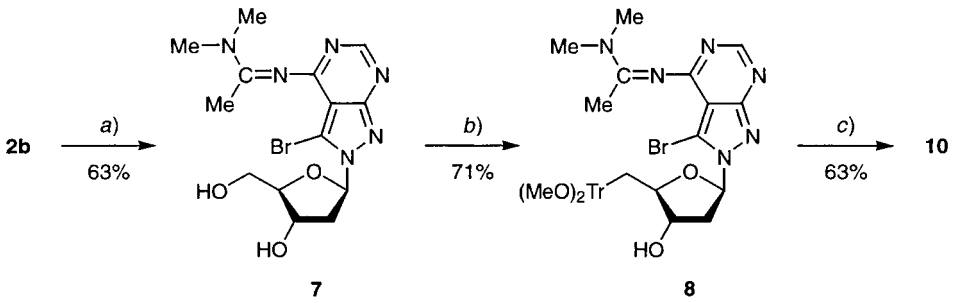

a) $Me_2NC(Me)(OMe)_2$, MeOH, 50°, 3 h. *b*) $(MeO)_2$Tr-Cl, pyridine, 50°, 2 h. *c*) $(i\text{-}Pr)_2NP(Cl)O(CH_2)_2CN$, CH_2Cl_2, 30 min, r.t.

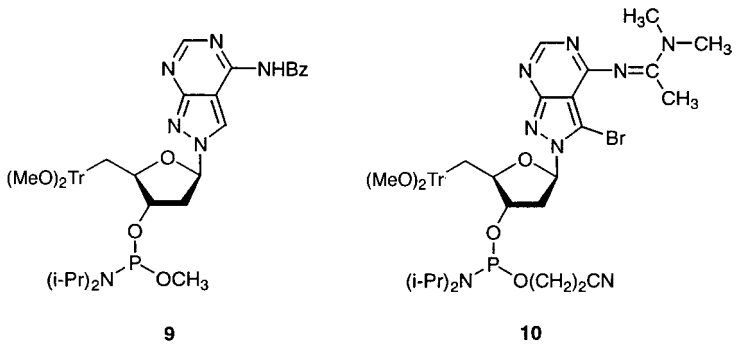

nol/Et_3N/dioxane 1:1:2 [10][25]. The homogeneity of the obtained oligonucleotides **11**–**39** (see below, *Tables 5*–*9*), was established by reversed-phase HPLC. MALDI-TOF-MS were measured (see *Exper. Part Table 10*), and the nucleoside composition

Table 4. *^{13}C-NMR Chemical Shifts of the 8-Aza-7-deazaadenine 2′-Deoxyribonucleoside Derivatives*[a])

	C(7)[b]) C(3)[c])	C(5)[b]) C(3a)[c])	C(6)[b]) C(4)[c])	C(2)[b]) C(6)[c])	C(4)[b]) C(7a)[c])	C(1′)[b])	C(2′)[b])
1a	133.2	100.6	158.2	156.2	153.8	84.2	38.1
b	118.9	99.8	157.3	156.9	154.5	84.0	37.8
c	91.0	103.5	157.6	156.2	154.0	84.0	37.9
2a	124.0	101.4	159.5	156.7	159.6	90.5	[d])
b	107.5	101.8	158.7	158.8	157.2	88.5	38.4
c	81.2	106.0	159.5	159.2	156.3	89.6	38.4
7	109.2	107.8	162.8	163.2	159.2	88.5	[d])
8	109.0	108.1	163.0	163.1	163.1	87.4	[d])

	C(3′)	C(4′)	C(5′)	MeO	Me_2N	C=N	Me
1a	71.2	87.7	62.6				
b	70.8	87.7	62.3				
c	70.9	87.7	62.3				
2a	70.7	88.4	62.1				
b	70.8	87.5	62.2				
c	70.9	88.4	62.2				
7	70.9	87.5	62.2			34.3, 42.2	157.0	16.9
8	70.0	85.0	63.8	54.9	[d])	157.7	16.8

[a]) Measured in (D_6)DMSO. [b]) Purine numbering. [c]) Systematic numbering. [d]) Superimposed by DMSO.

was determined after digestion of the oligonucleotides with snake-venom phosphodiesterase followed by alkaline phosphatase. Representative examples confirming the nucleoside composition are shown in *Fig. 5*.

2.2. *Stability of Duplexes with Antiparallel Chain Orientation. Tables 5–9* summarize the T_m values and the thermodynamic data of a series of oligonucleotide duplexes. The data were determined by curve-shape analysis of the melting profiles (MeltWin; version 3.0) [27]. The duplexes 5′-d(A-T)$_6$ that contain 8-aza-7-deaza-2′-deoxyadenosine (**1a**) or its N^8-glycosylated isomer **2a** [10] in place of A_d are more stable than the parent 5′-d(A-T)$_6$ (see **12**·**12** and **13**·**13** *vs.* **11**·**11**) [10] (*Table 5*). While the T_m increase of the duplex **12**·**12** over that of the parent **11**·**11** is rather small ($\Delta T_m = 3°$), the duplex **13**·**13** is very stable ($\Delta T_m = 16°$). The homomeric duplexes **16**·**15** or **17**·**15** (*Table 5*) show slightly lower T_m values than the parent duplex **14**·**15**. Only duplexes that are composed of tracts of N^8-linked 'purines' and pyrimidines within the same strand are not as stable as those with a regular glycosylation position (compare **20**·**20** with **18**·**18** or **19**·**19**).

The CD spectrum of the duplex **13**·**13** formed by the alternating residues **2a** and T_d is different to that of the duplex **11**·**11** formed by **1a** and T_d (*Fig. 6,a*). The modified duplex shows a negative *Cotton* effect at 305 nm: the negative *Cotton* effect of 5′-d(A-T)$_6$-3′ at 245 nm is absent. Similar CD changes are observed in the case of oligonucleotide duplexes of homomeric and block oligonucleotides (*Fig. 6,b* and *c*). While the CD spectra of the oligonucleotides **16**·**15** and **19**·**19** containing N^9-glycosylated 8-aza-7-deaza-2′-deoxyadenosine (**1a**) show similarities to the parent 'adenine' oligonucleotides **14**·**15** or **18**·**18**, respectively, the duplexes **17**·**15** and **20**·**20** containing the N^8-glycosylated compound **2a** are bathochromically shifted. To show the

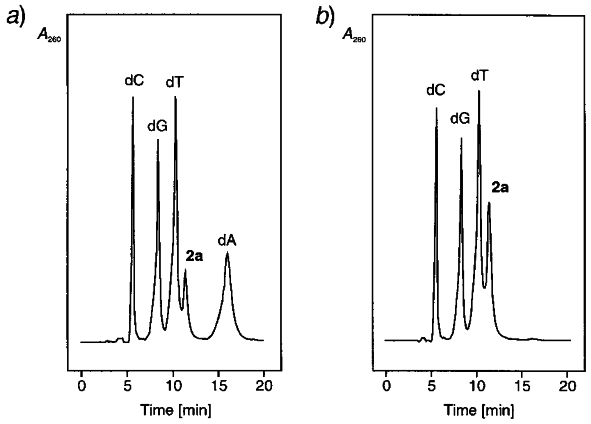

Fig. 5. *Reversed-phase HPLC profiles of the hydrolysis products of* a) *5′-d(T-A-G-G-T-C-***2a-2a***-T-A-C-T)-3′* (**24**) *and* b) *5′-d(T-***2a***-G-G-T-C-***2a-2a***-T-***2a***-C-T)-3′* (**25**) *formed by snake-venom phosphodiesterase followed by alkaline phosphatase.* Conditions, see *Exper. Part.*

Table 5. T_m *Values and Thermodynamic Data of the Oligonucleotides Containing 8-Aza-7-deaza-2′-deoxyadenosine* (**1a**) *and the* N^8*-Glycosylated Nucleoside* **2a**

	T_m [°][a])	ΔH^0 [kcal/mol]	ΔS^0 [cal/mol · K]	ΔG^0_{298} [kcal/mol]
5′-d[(A-T-A-T-A-T-A-T-A-T-A-T)]$_2$-3′ (**11**·**11**)	33 (26)	−45 (−44)	−125 (−127)	−6.3 (−5.5)
5′-d[(**1a**-T-**1a**-T-**1a**-T-**1a**-T-**1a**-T-**1a**-T)]$_2$-3′ (**12**·**12**) [10]	36	−63	−180	−7.2
5′-d[(**2a**-T-**2a**-T-**2a**-T-**2a**-T-**2a**-T-**2a**-T)]$_2$-3′ (**13**·**13**) [10]	49 (39)	−74 (−62)	−207 (−175)	−9.6 (−7.3)
	41[c]) (22)[d])	−62 (−23)	−175 (−54)	−7.8 (−5.9
5′-d(A_{12})-3′·3′-d(T_{12})-5′ (**14**·**15**) [28]	44 (37)	−84 (−91)	−238 (−267)	−9.8 (−7.9)
5′-d(**1a**$_{11}$-A)-3′·3′-d(T_{12})-5′ (**16**·**15**) [28]	38 (32)	−91 (−65)	−266 (−186)	−8.4 (−6.8)
5′-d(**2a**$_{12}$)-3′·3′-d(T_{12})-5′ (**17**·**15**)	38 (31)	−68 (−78)	−195 (−232)	−7.8 (−6.3)
5′-d[(A_6-T_6)]$_2$-3′ (**18**·**18**) [28]	46 (40)	−81 (−75)	−232 (−219)	−9.1 (−7.4)
5′-d[(**1a**$_6$-T_6)]$_2$-3′ (**19**·**19**) [28]	44 (39)	−49 (−58)	−133 (−163)	−8.3 (−7.1)
5′-d[(**2a**$_6$-T_6)]$_2$-3′ (**20**·**20**)	25 (17)	[b])	[b])	[b])

[a]) Measured at 260 nm. Data without parentheses are measured in 1M NaCl containing 100 mM $MgCl_2$ and 60 mM Na-cacodylate (pH 7.0) with 10 μM oligonucleotide concentration. Data in parentheses are measured in 100 mM NaCl, 10 mM $MgCl_2$, and 10 mM Na-cacodylate (pH 7.0) with 10 μM oligonucleotide concentration. [b]) Not determined. [c]) 1M NaCl, 10 mM Na-phosphate, and 0.1 mM EDTA (pH 7.0). [d]) 10 mM NaCl, 10 mM Na-phosphate, and 0.1 mM EDTA (pH 7.0).

structural characteristics of oligonucleotide exclusively due to residue **2a**, the CD spectrum of homomer **17** was measured and compared with that of d(A_{12}) [28]; the significant differences in these spectra are due to the conformational properties of the monomers. When the single-stranded oligomer **17** was hydrolyzed with snake-venom phosphodiesterase and alkaline phosphatase, the UV spectrum of the monomer **2a** was obtained (*Fig. 7,a*). According to the pronounced differences observed in the CD spectra of the homomer **17** and the monomer **2a** (*Fig. 7,b*), the single strands have a

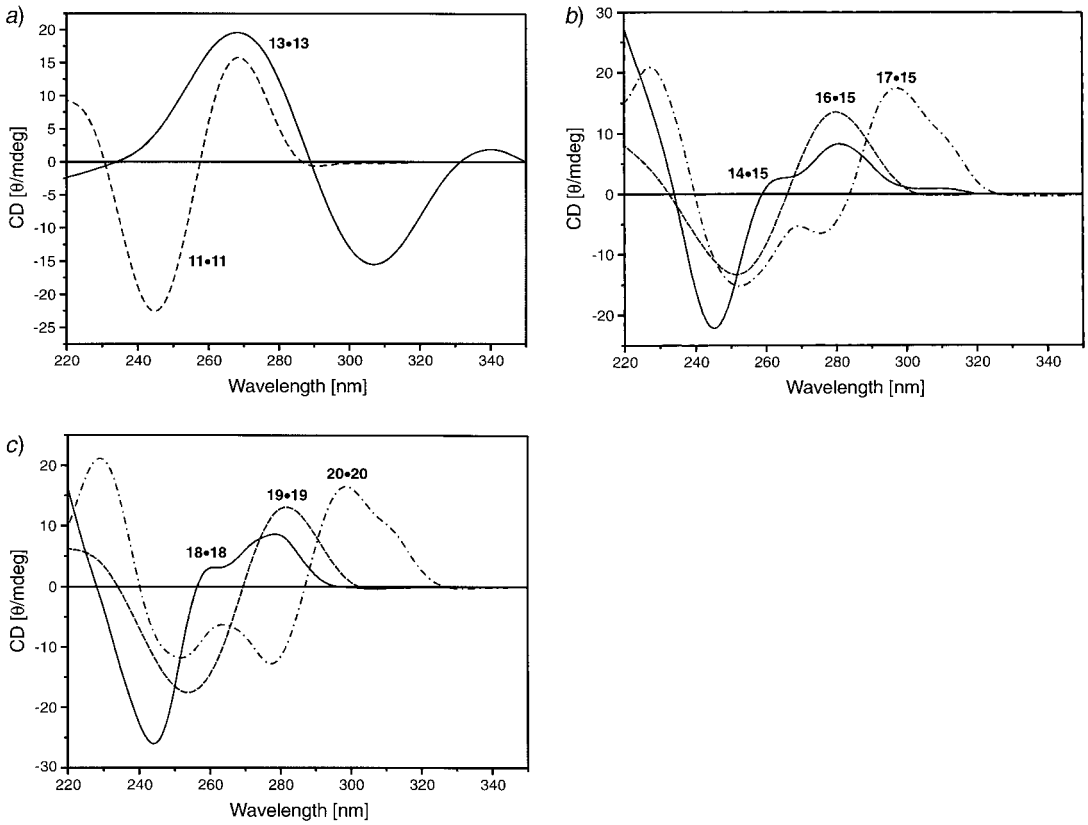

Fig. 6. a) *CD Spectra of the alternating 12-mer duplexes* **11**·**11** *and* **13**·**13**; b) *CD spectra of the homomeric duplexes* **14**·**15**, **16**·**15**, *and* **17**·**15**; c) *CD spectra of the block oligomers* **18**·**18**, **19**·**19**, *and* **20**·**20**. Spectra were measured at 10° in 1M NaCl, 100 mM $MgCl_2$, and 60 mM Na-cacodylate (pH 7.0) with 10 μM oligomer concentration. For sequences, see *Table 5*.

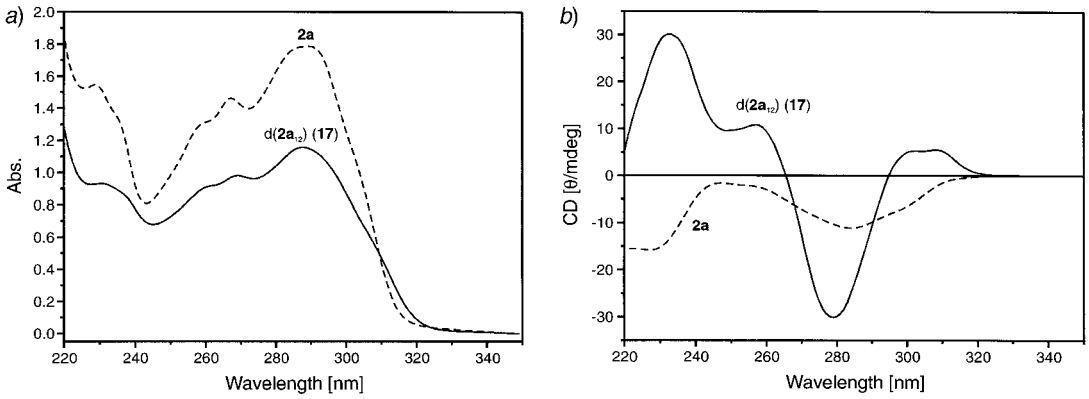

Fig. 7. a) *UV Spectra and* b) *CD spectra of the homomeric oligonucleotide d(***2a**$_{12}$*)* (**17**) *before and after enzymatic digestion*. Measured at 10° in bidistilled water.

well-organized structure. This is due to stacking interactions between the base residues reflected by a hypochromicity of 35% (289 nm) determined by the enzymatic hydrolyses of the oligomer d(**2a**)$_{12}$.

Next, a series of oligonucleotides with random base composition was synthesized. They are derived from the oligomers 5′-d(T-A-G-G-T-C-A-A-T-A-C-T)-3′ (**21**) and 3′-d(A-T-C-C-A-G-T-T-A-T-G-A)-5′ (**22**), which are commonly used in our laboratory to study the influence of modified bases on the duplex stability. When two 2′-deoxyadenosine residues of the duplex **21**·**22** are replaced by compound **2a**, a decrease of the T_m value of only 1° per incorporated N^8-nucleoside residue results (see **23**·**22**), while a decrease of 3° per residue is observed in the case of duplex **24**·**22** (see *Table 6*). This indicates the dependence of the duplex stability on the incorporation position of residue **2a**. Furthermore, the incorporation at some positions of duplex **21**·**22** is more sensitive than at others. When two residues **2a** replace A_d, resulting in the duplexes **23**·**22**, **24**·**22**, and **21**·**28**, the decrease of the T_m value changes from 2° to 12° when compared with the parent duplex **21**·**22**. From the T_m data of *Table 6*, it can also be seen that the duplex stability is strongly affected when both strands are modified (see **23**·**28**, **24**·**28**, and **25**·**28**). Nevertheless, the destabilization caused by the incorporation of the N^8-linked nucleoside **2a** in one strand is rather small compared to the effect of residues causing real mismatches (ΔT_m/mismatch > 10°). The CD spectra of some duplexes of *Table 6* are given in *Fig. 8*.

The T_m values were also measured in Mg^{2+}-free buffer solution at various concentrations of NaCl. According to *Table 7*, the salt dependence of the T_m values of a duplex containing A_d (**21**·**22**) with those containing the modified nucleoside **2a** shows an almost identical behavior. The stability of the unmodified DNA·RNA hybrid **21**·**38** (T_m 46°, *Table 8*) is slightly lower than that of the DNA·DNA duplex **21**·**22** (T_m 47°, *Table 7*). However, when compound **2a** is replacing 2′-deoxyadenosine (see **23**·**38**, **24**·**38**, and **25**·**38**), the T_m decrease is rather important (*Table 8*).

2.3. *Stability of Parallel-Stranded Duplexes.* The influence of the N^8-linked nucleoside **2a** on duplexes with parallel-strand (ps) orientation was also studied. For this purpose, the oligodeoxynucleotide **39**, wherein guanine is replaced by isoguanine and cytosine by 5-methylisocytosine, was chosen (*Table 9*) [29]. According to *Table 9*, the incorporation of the nucleoside **2a** reduces the T_m values (see **23**·**39** and **24**·**39** *vs.* **21**·**39**), as it is observed for the duplexes with antiparallel-strand (aps) orientation. Interestingly, the ΔT_m between modified and unmodified duplexes is larger in the case of ps-hybrids (*Table 9*) than in the case of aps duplexes (see **23**·**22** and **24**·**22** *vs.* **21**·**22** in *Table 6*). A comparison of the ΔG^0_{298} values of the modified aps or ps duplexes with their unmodified counterparts, determined in 1M NaCl, 100 mM $MgCl_2$, 60 mM Na-cacodylate, indicates a decrease of $|\Delta G^0_{298}|$ upon modification; *e.g.*, the aps duplex **23**·**22** or the ps duplex **23**·**39**, compared with the unmodified duplexes **21**·**22** or **21**·**39**, respectively, show a $\Delta\Delta G^0_{298}$ of 1.3 and 1.9 kcal/mol, respectively. If another sequence is chosen but the number of substitutions is the same (*e.g.* 2), different $\Delta\Delta G^0_{298}$ values are calculated; 2.3 kcal/mol for **24**·**22** in comparison to **21**·**22** and 2.8 kcal/mol for **24**·**39** in comparison to **21**·**39**. This indicates that the decrease of ΔG^0 upon incorporation of **2a** depends on the position of the modification. However, this dependence seems to be rather similar in aps- and ps-DNA, a finding that was not expected.

Table 6. T_m *Values and Thermodynamic Data of the Oligonucleotides Containing* N^8*-Linked 8-Aza-7-deaza-adenine 2′-Deoxyribonucleoside* **2a** *and its 7-Bromo Derivative* **2b**

	T_m [°][a])	ΔH^0 [kcal/mol]	ΔS^0 [cal/mol · K]	ΔG^0_{298} [kcal/mol]
5′-d(T-A-G-G-T-C-A-A-T-A-C-T)-3′ (**21**) 3′-d(A-T-C-C-A-G-T-T-A-T-G-A)-5′ (**22**)	50 (47)	− 90 (− 89)	− 252 (− 253)	− 11.8 (− 10.9)
5′-d(T-**2a**-G-G-T-C-A-A-T-**2a**-C-T)-3′ (**23**) 3′-d(A-T-C-C-A-G-T-T-A-T-G-A)-5′ (**22**)	48 (44)	− 80 (− 78)	− 224 (− 222)	− 10.5 (− 9.6)
5′-d(T-A-G-G-T-C-**2a-2a**-T-A-C-T)-3′ (**24**) 3′-d(A-T-C-C-A-G-T-T-A-T-G-A)-5′ (**22**)	44 (41)	− 79 (− 82)	− 224 (− 236)	− 9.5 (− 8.9)
5′-d(T-**2a**-G-G-T-C-**2a-2a**-T-**2a**-C-T)-3′ (**25**) 3′-d(A-T-C-C-A-G-T-T-A-T-G-A)-5′ (**22**)	41 (39)	− 78 (− 78)	− 222 (− 224)	− 8.8 (− 8.5)
5′-d(T-A-G-G-T-C-A-A-T-A-C-T)-3′ (**21**) 3′-d(A-T-C-C-**2a**-G-T-T-A-T-G-A)-5′ (**26**)	46 (42)	− 77 (− 81)	− 217 (− 231)	− 9.8 (− 9.1)
5′-d(T-A-G-G-T-C-A-A-T-A-C-T)-3′ (**21**) 3′-d(A-T-C-C-A-G-T-T-**2a**-T-G-A)-5′ (**27**)	45 (42)	− 70 (− 72)	− 194 (− 204)	− 9.5 (− 8.8)
5′-d(T-A-G-G-T-C-A-A-T-A-C-T)-3′ (**21**) 3′-d(A-T-C-C-**2a**-G-T-T-**2a**-T-G-A)-5′ (**28**)	38 (34)	− 57 (− 50)	− 158 (− 138)	− 7.8 (− 7.0)
5′-d(T-**2a**-G-G-T-C-A-A-T-**2a**-T-T)-3′ (**23**) 3′-d(A-T-C-C-**2a**-G-T-T-**2a**-T-G-A)-5′ (**28**)	33 (27)	− 48 (− 37)	− 122 (− 99)	− 6.8 (− 6.3)
5′-d(T-A-G-G-T-C-**2a-2a**-T-A-C-T)-3′ (**24**) 3′-d(A-T-C-C-**2a**-G-T-T-**2a**-T-G-A)-5′ (**28**)	27 (24)	− 45 (− 40)	− 126 (− 110)	− 6.2 (− 5.7)
5′-d(T-**2a**-G-G-T-C-**2a-2a**-T-**2a**-C-T)-3′ (**25**) 3′-d(A-T-C-C-**2a**-G-T-T-**2a**-T-G-A)-5′ (**28**)	25 (21)	− 48 (− 56)	− 136 (− 168)	− 5.7 (− 4.2)
5′-d(C-G-A-A-C-T-G-G-C-G-T-C)-3′ (**29**) 3′-d(G-C-T-T-G-A-C-C-G-C-A-G)-5′ (**30**)	62 (61)	− 99 (− 96)	− 270 (− 263)	− 15.1 (− 14.6)
5′-d(C-G-A-A-C-T-G-G-C-G-T-C)-3′ (**29**) 3′-d(G-C-T-T-G-**2a**-C-C-G-C-**2a**-G)-5′ (**31**)	57 (57)	− 97 (− 100)	− 267 (− 279)	− 13.7 (− 13.8)
5′-d(C-G-**2a-2a**-C-T-G-G-C-G-T-C)-3′ (**32**) 3′-d(G-C-T-T-G-A-C-C-G-C-A-G)-5′ (**30**)	54 (53)	− 72 (− 71)	− 195 (− 192)	− 11.4 (− 11.1)
5′-d(C-G-**2a-2a**-C-T-G-G-C-G-T-C)-3′ (**32**) 3′-d(G-C-T-T-G-**2a**-C-C-G-C-**2a**-G)-5′ (**31**)	50 (50)	− 81 (− 86)	− 225 (− 240)	− 11.0 (− 11.3)
5′-d(T-**2b**-G-G-T-C-A-A-T-**2b**-C-T)-3′ (**33**) 3′-d(A-T-C-C-A-G-T-T-A-T-G-A)-5′ (**22**)	46	− 75	− 210	− 9.8
5′-d(T-A-G-G-T-C-A-A-T-A-C-T)-3′ (**21**) 3′-d(A-T-C-C-**2b**-G-T-T-**2b**-T-G-A)-5′ (**34**)	32	− 40	− 107	− 6.9
5′-d(T-**2b**-G-G-T-C-A-A-T-**2b**-C-T)-3′ (**33**) 3′-d(A-T-C-C-**2b**-G-T-T-**2b**-T-G-A)-5′ (**34**)	24	− 30	− 78	− 5.9
5′-d(T-**1b**-G-G-T-C-**1b-1b**-T-**1b**-C-T)-3′ (**35**) [27] 3′-d(A-T-C-C-**2b**-G-T-T-**2b**-T-G-A)-5′ (**34**)	28	− 42	− 114	− 6.5
5′-d(T-**1c**-G-G-T-C-**1c-1c**-T-**1c**-C-T)-3′ (**36**) [27] 3′-d(A-T-C-C-**2b**-G-T-T-**2b**-T-G-A)-5′ (**34**) [27]	37	− 45	− 119	− 7.7
5′-d(T-**1b**-G-G-T-C-**1b-1b**-T-**1b**-C-T)-3′ (**35** 3′-d(A-T-C-C-**1b**-G-T-T-**1b**-T-G-A)-5′ (**37**)	61	[b])	[b])	[b])

[a]) Measured at 260 nm in 1M NaCl, 100 mM $MgCl_2$, and 60 mM Na-cacodylate (pH 7.0) with 5 μM single-strand concentration. Data in parentheses are measured in 100 mM NaCl, 10 mM $MgCl_2$, and 10 mM Na-cacodylate (pH 7.0) with 10 μM oligonucleotide concentration. [b]) Not determined.

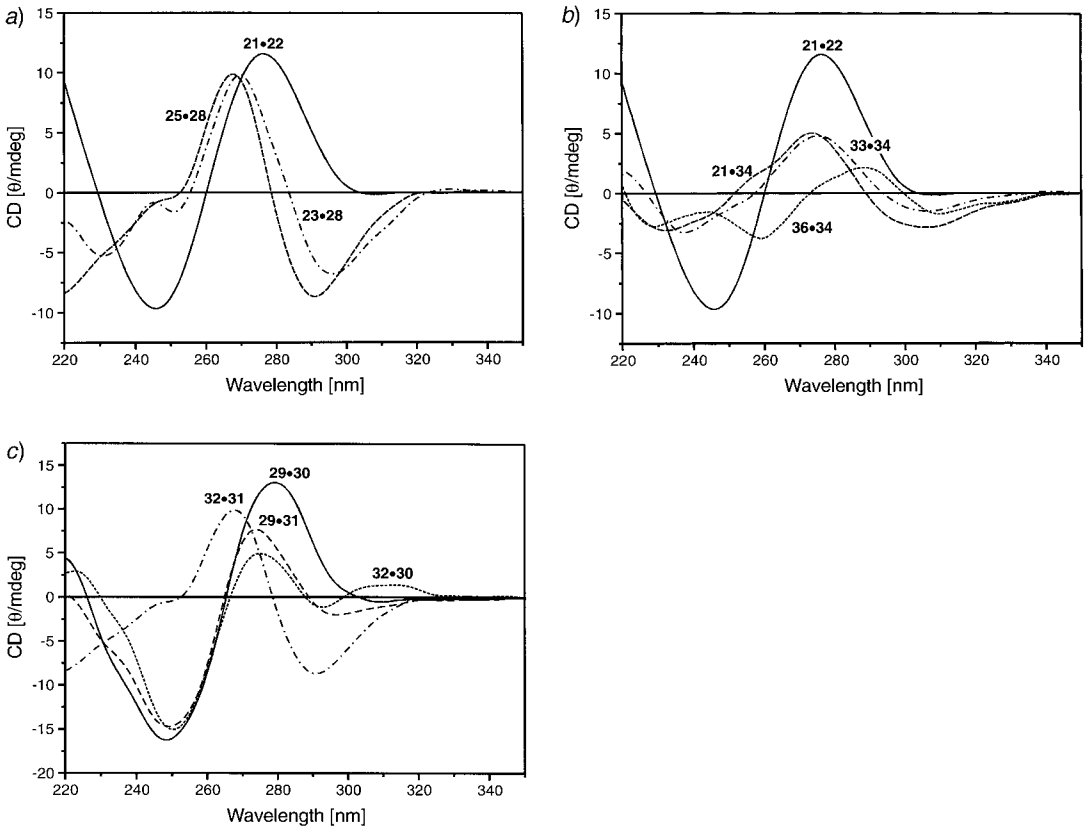

Fig. 8. a) *CD Spectra of the oligonucleotides* **21** · **22**, **23** · **28**, *and* **25** · **28**; b) *CD spectra of the oligomers* **21** · **34**, **33** · **34**, *and* **36** · **34**; c) *CD spectra of the oligonucleotides* **29** · **30**, **29** · **31**, **32** · **30**, *and* **32** · **31**. Spectra were measured in 1M NaCl, 100 mM $MgCl_2$, and 60 mM Na-cacodylate (pH 7.0) with 5 + 5 μM oligonucleotide concentration.

Table 7. T_m *Values of Oligonucleotides Containing* N^8*-Linked-8-Aza-7-deazaadenine 2′-Deoxyribonucleoside* **2a** *Measured in* Mg^{2+}*-Free Buffers*[a])

	T_m [°][b])	T_m [°][c])	T_m [°][d])
5′-d(T-A-G-G-T-C-A-A-T-A-C-T)-3′ (**21**) 3′-d(A-T-C-C-A-G-T-T-A-T-G-A)-5′ (**22**)	53	43	40
5′-d(T-**2a**-G-G-T-C-A-A-T-**2a**-C-T)-3′ (**23**) 3′-d(A-T-C-C-A-G-T-T-A-T-G-A)-5′ (**22**)	49	38	34
5′-d(T-A-G-G-T-C-**2a-2a**-T-A-C-T)-3′ (**24**) 3′-d(A-T-C-C-A-G-T-T-A-T-G-A)-5′ (**22**)	43	34	30
5′-d(T-**2a**-G-G-T-C-**2a-2a**-T-**2a**-C-T)-3′ (**25**) 3′-d(A-T-C-C-A-G-T-T-A-T-G-A)-5′ (**22**)	40	31	27
5′-d(T-A-G-G-T-C-A-A-T-A-C-T)-3′ (**21**) 3′-d(A-T-C-C-**2a**-G-T-T-**2a**-T-G-A)-5′ (**28**)	37	24	20

[a]) Measured at 260 nm. [b]) 1M NaCl, 10 mM Na-phosphate, and 0.1 mM EDTA. [c]) 100 mM NaCl, 10 mM Na-phosphate, and 0.1 mM EDTA. [d]) 50 M NaCl, 10 mM Na-phosphate, and 0.1 mM EDTA.

Table 8. T_m *Values and Thermodynamic Data of the DNA/RNA Hybrids Containing* N^8*-Linked 8-Aza-7-deaza-adenine 2′-Deoxyribonucleoside* **2a**[a])

	T_m [°][a])	ΔH^0 [kcal/mol]	ΔS^0 [cal/mol · K]	ΔG^0_{298} [kcal/mol]
5′-d(T-A-G-G-T-C-A-A-T-A-C-T)-3′ (**21**) [28] 3′-(A-U-C-C-A-G-U-U-A-U-G-A)-5′ (**38**)	46	– 82	– 230	– 10.1
5′-d(T-**2a**-G-G-T-C-A-A-T-**2a**-C-T)-3′ (**23**) 3′-(A-U-C-C-A-G-U-U-A-U-G-A)-5′ (**38**)	37	– 66	– 189	– 7.1
5′-d(T-A-G-G-T-C-**2a-2a**-T-A-C-T)-3′ (**24**) 3′-(A-U-C-C-A-G-U-U-A-U-G-A)-5′ (**38**)	33	– 61	– 178	– 7.1
5′-d(T-**2a**-G-G-T-C-**2a-2a**-T-**2a**-C-T)-3′ (**25**) 3′-(A-U-C-C-A-G-U-U-A-U-G-A)-5′ (**38**)	22	– 40	– 112	– 5.9

[a]) Measured at 260 nm in 0.1M NaCl, 10 mM $MgCl_2$, and 10 mM Na-cacodylate (pH 7.0) with 5 μM single-strand concentration.

Table 9. T_m *Values and Thermodynamic Data of the Oligonucleotides Containing* N^8*-Linked 8-Aza-7-deazaadenine 2′-Deoxyribonucleoside* **2a** *in Parallel-Stranded DNA*[a]). d(iC) = m^5iC_d

	T_m [°]	ΔH^0 [kcal/mol]	ΔS^0 [cal/mol · K]	ΔG^0_{298} [kcal/mol]
5′-d(T-A-G-G-T-C-A-A-T-A-C-T)-3′ (**21**) 5′-d(A-T-iC-iC-A-iG-T-T-A-T-iG-A)-3′ (**39**) [29]	39	– 74	– 211	– 8.8
5′-d(T-**2a**-G-G-T-C-A-A-T-**2a**-C-T)-3′ (**23**) 5′-d(A-T-iC-iC-A-iG-T-T-A-T-iG-A)-3′ (**39**)	33	– 50	– 138	– 6.9
5′-d(T-A-G-G-T-C-**2a-2a**-T-A-C-T)-3′ (**24**) 5′-d(A-T-iC-iC-A-iG-T-T-A-T-iG-A)-3′ (**39**)	28	– 49	– 140	– 6.0

[a]) Measured at 260 nm in 1M NaCl containing 100 mM $MgCl_2$ and 60 mM Na-cacodylate (pH 7.0) with 10 μM oligonucleotide concentration.

3. *Base-Pair Motifs and Conclusion*. The nucleoside **2a** forms a rather strong base pair with thymidine in aps-DNA, while that in ps-DNA is less stable. The most likely base-pair motifs are a reverse *Watson-Crick* base pair for **2a** with T_d in aps-DNA (motif **I**) and a *Watson-Crick* pair in ps-DNA (motif **III**; *Fig. 9*). The distances of the two anomeric centers within these base pairs are rather similar (motif **I** *vs.* **II** or motiv **III** *vs.* **IV**) [30]. However, the glycosylic-bond angles are different in motif **I** (O(4′)–C(1′)–N(8)–N(9)) compared to motif **II** (O(4′)–C(1′)–N(9)–C(4)). The glycosylic-torsion angle of the N^8-nucleoside **2a** in base pair **I** is in the *syn* range. The amino group of motif **I** points towards the minor groove and not towards the major groove as observed for *Watson-Crick* base pairs (see motif **II**). Consequently, substituents at C(7) also point towards the minor groove (motif **I**) and not towards the major groove (motif **II**). According to the limitation of space of the minor groove, bulky 7-substituents should destabilize the duplex. This is actually the case, as the incorporation of the bromo nucleoside **2b** destabilizes the duplex in comparison to that containing **2a** (*Table 6*).

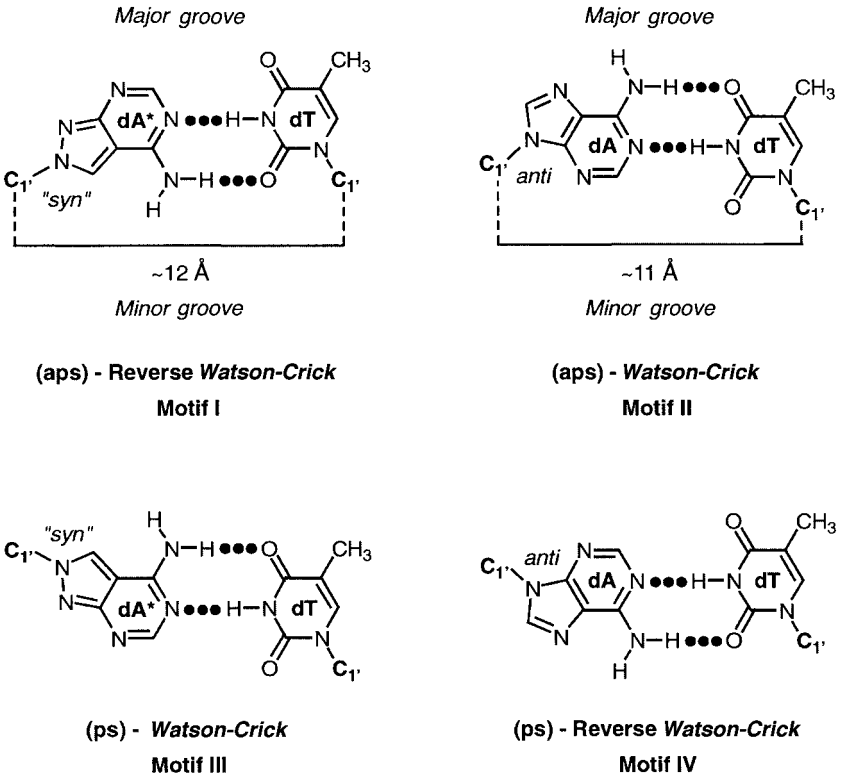

Fig. 9. *Comparison of the base-pair motifs of* **2a** (dA*) *with those of regular* A_d (dA) *in antiparallel-strand* (aps) *and parallel-strand orientation* (ps)

Experimental Part

General. All chemicals were purchased from *Aldrich*, *Sigma*, or *Fluka* (*Sigma-Aldrich Chemie GmbH*, Deisenhofen, Germany). Solvents were of laboratory grade. TLC: aluminum sheets, silica gel *60* F_{254}, 0.2 mm layer (*Merck*, Germany). Column flash chromatography (FC): silica gel *60* (*Merck*, Germany) at 0.4 bar ($4 \cdot 10^4$ Pa); solvent systems: CH_2Cl_2/MeOH 9:1 (*A*), CH_2Cl_2/MeOH 8:2 (*B*), petroleum ether/acetone 1:2 (*C*), CH_2Cl_2/acetone 8:2 (*D*), CH_2Cl_2/acetone 9:1 (*E*); sample collection with an *UltroRac II* fractions collector (*LKB Instruments*, Sweden). M.p.: *Büchi-SMP-20* apparatus (*Büchi*, Switzerland); uncorrected. UV Spectra: *U-3200* spectrometer (*Hitachi*, Japan). NMR Spectra: *Avance-250* or *AMX-500* spectrometers (*Bruker*, Karlsruhe, Germany), at 250.13 and 500.14 MHz for ^{1}H and at 125.13 MHz for ^{13}C; δ in ppm rel. to $SiMe_4$ as internal standard, *J* values in Hz. Positive-ion fast-atom-bombardment (FAB) mass spectra were provided by Dr. *M. Sauer* (Universität Heidelberg, Germany) using 3-nitrobenzyl alcohol (3-NOBA) as matrix. Elemental analyses were performed by *Mikroanalytisches Laboratorium Beller* (Göttingen, Germany).

*3-Bromo-2-[2-deoxy-β-*D-erythro-*pentofuranosyl]-2*H-*pyrazolo[3,4-*d*]pyrimidin-4-amine* (**2b**). Compound **5b** (1.0 g, 1.72 mmol) [13] was stirred at 80° for 6 h with sat. (0°) NH_3/MeOH soln. (200 ml) in an autoclave. The soln. was evaporated and the residue applied to FC (column 12×3 cm, solvent *B*): **2b** (259 mg, 44%). Colorless amorphous powder. TLC (*A*): 0.17. UV (MeOH): 244 (9200), 262 (8200), 303 (9200). ^{1}H-NMR ((D_6)DMSO): 2.34 (*m*, 1 H–C(2′)); 2.91 (*m*, 1 H–C(2′)); 3.45 (*m*, 2 H–C(5′)); 3.85 (*m*, H–C(4′)); 4.50 (*m*, H–C(3′)); 4.76 (*t*, *J* = 5.7, OH–C(5′)); 5.36 (*d*, *J* = 4.5, OH–C(3′)); 6.44 (‘*t*’, *J* = 5.7, H–C(1′)); 7.29 (br. *s*, NH_2); 8.19 (*s*, H–C(6)). Anal. calc. for $C_{10}H_{12}BrN_5O_3$ (330.14): C 36.38, H 3.66, N 21.21; found: C 36.48, H 3.52, N 21.17.

2-[2-Deoxy-β-D-erythro-*pentofuranosyl]-3-iodo-2*H-*pyrazolo[3,4-*d*]pyrimidin-4-amine* (**2c**). As described for **2b**, with **5c** (200 mg, 0.32 mmol) [13] and NH_3/MeOH soln. (200 ml). After FC, crystallization from MeOH/H_2O furnished **2c** (60 mg, 48%). Colorless solid. M.p. 208–211°. TLC (*A*): 0.15. UV (MeOH): 248 (6900), 266 (7900), 274 (8000), 307 (9200). ^{1}H-NMR ((D_6)DMSO): 2.33 (*m*, 1 H–C(2′)); 2.90 (*m*, 1 H–C(2′)); 3.42 (*m*, 2 H–C(5′)); 3.87 (*m*, H–C(4′)); 4.50 (*m*, H–C(3′)); 4.79 (‘*t*’, *J* = 5.6, OH–C(5′)); 5.36 (*d*, *J* = 4.6, OH–C(3′)); 6.43 (‘*t*’, *J* = 5.8, H–C(1′)); 7.30 (br. *s*, NH_2); 8.19 (*s*, H–C(6)). Anal. calc. for $C_{10}H_{12}IN_5O_3$ (377.14): C 31.85, H 3.21, N 18.57; found: C 32.08, H 3.13, N 18.44.

3-Bromo-2-(2-deoxy-β-D-erythro-*pentofuranosyl)-4-[(dimethylamino)ethylidene]-2*H-*pyrazolo[3,4-*d*]pyrimidin-4-amine* (**7**). A soln. of **2b** (200 mg, 0.61 mmol) in MeOH (10 ml) was stirred with *N*,*N*-dimethylacetamide dimethyl acetal (2.0 g) for 3 h at 50°. After evaporation, the residue was applied to FC (column 12 × 3 cm, solvent *B*): **7** (152 mg, 62%). Colorless foam. TLC (*A*): 0.28. UV (MeOH): 275 (8500), 329 (14900). ^{1}H-NMR ((D_6)DMSO): 2.29 (*s*, 1 Me); 2.36 (*m*, 1 H–C(2′)); 2.87 (*m*, 1 H–C(2′)); 3.19 (*s*, MeN); 3.21 (*s*, MeN); 3.49 (*m*, 2 H–C(5′)); 3.86 (*m*, H–C(4′)); 4.51 (*m*, H–C(3′)); 4.78 (‘*t*’, *J* = 5.4, OH–C(5′)); 5.37 (*d*, *J* = 4.6, OH–C(3′)); 6.49 (‘*t*’, *J* = 5.7, H–C(1′)); 8.41 (*s*, H–C(6)).

*3-Bromo-2-[2-deoxy-5-*O*-(4,4′-dimethoxytriphenylmethyl)-β*-D-erythro-*pentofuranosyl]-4-[(dimethylamino)ethylidene]-2*H-*pyrazolo[3,4-*d*]pyrimidin-4-amine* (**8**). To a soln. of **7** (140 mg, 0.35 mmol) in dry pyridine (0.5 ml), 4,4′-dimethoxytriphenylmethyl chloride (130 mg, 0.38 mmol) was added. After stirring at 50° for 2 h, the mixture was poured into an ice-cold 3% aq. $NaHCO_3$ soln. (5 ml) and extracted with CH_2Cl_2 (2 × 75 ml). The combined org. layers were dried (Na_2SO_4) and evaporated. The residue was applied to FC (column 15 × 2 cm, solvent *A*): **8** (175 mg, 71%). Colorless foam. TLC (*A*): 0.51. UV (MeOH): 275 (10900), 335 (12700). ^{1}H-NMR ((D_6)DMSO): 2.26 (*s*, 1 CH_3); 2.38 (*m*, 1 H–C(2′)); 2.90 (*m*, 1 H–C(2′)); 3.03 (*m*, 2 H–C(5′)); 3.17 (*s*, MeN); 3.23 (*s*, MeN); 3.68 (*s*, MeO); 3.69 (*s*, MeO); 3.93 (*m*, H–C(4′)); 4.64 (*m*, H–C(3′)); 5.40 (*d*, *J* = 5.1, OH–C(3′)); 6.58 (*dd*, *J* = 5.4, H–C(1′)); 6.75 (*m*, $(MeO)_2$*Tr*); 7.10–7.38 (*m*, $(MeO)_2$*Tr*); 8.40 (*s*, H–C(6)). Anal. calc. for $C_{35}H_{37}BrN_6O_5$ (701.62): C 59.92, H 5.32, N 11.98; found: C 60.21, H 4.97, N 11.60.

*3-Bromo-2-[2-deoxy-5-*O*-(4,4′-dimethoxytriphenylmethyl)-β*-D-erythro-*pentofuranosyl]-4-[(dimethylamino)ethylidene]-2*H-*pyrazolo[3,4-*d*]pyrimidin-4-amine 3′-(2-Cyanoethyl Diisopropylphosphoramidite)* (**10**). To a stirred soln. of dry **8** (150 mg, 0.21 mmol) and anh. ^{i}Pr$_2$EtN (80 mg, 0.63 mmol) in dry THF (1 ml), 2-cyanoethyl diisopropylphosphoramidochloridite (65 mg, 0.28 mmol) was added under Ar. The mixture was stirred for 30 min and then filtered. The filtrate was diluted with AcOEt (80 ml) and extracted twice with an ice-cold 3% aq. $NaHCO_3$ soln. (2 × 10 ml) and H_2O (2 × 10 ml). The org. phase was dried (Na_2SO_4) and evaporated. The residue was applied to FC (column 12 × 2 cm, solvent *C*): **10** (120 mg, 63%). Colorless oil. TLC (*C*) 0.3, 0.4. ^{31}P-NMR ($CDCl_3$): 150.4.

Table 10. *Molecular Masses Determined by MALDI-TOF Mass Spectroscopy of the Modified Oligonucleotides Containing $c^7z^8A_d$* (***2a***) and its 7-Bromo-Derivative $Br^7c^7z^8A_d$* (***2b***)*

	M^+ (calc.)	M^+ (found)
5′-d(**2a**-T-**2a**-T-**2a**-T-**2a**-T-**2a**-T)-3′ (**13**)	3640.7	3638.8
5′-d(T-**2a**-G-G-T-C-A-A-T-**2a**-C-T)-3′ (**23**)	3642.7	3641.7
5′-d(T-A-G-G-T-C-**2a-2a**-T-A-C-T)-3′ (**24**)	3642.7	3642.2
5′-d(T-**2a**-G-G-T-C-**2a-2a**-T-**2a**-C-T)-3′ (**25**)	3642.7	3642.1
5′-d(A-G-T-**2a**-T-T-G-**2a**-C-C-T-A)-3′ (**28**)	3642.7	3641.5
5′-d(G-**2a**-C-G-C-C-**2a**-G-T-T-C-G)-3′ (**31**)	3644.7	3643.3
5′-d(C-G-**2a-2a**-C-T-G-G-C-G-C-T)-3′ (**32**)	3644.7	3643.5
5′-d(T-**2b**-G-G-T-C-A-A-T-**2b**-C-T)-3′ (**33**)	3798.5	3800.4
5′-d(A-G-T-**2b**-T-T-G-**2b**-C-C-T-A)-3′ (**34**)	3798.5	3802.5

Synthesis and Purification of the Oligonucleotides **11**–**39**. The oligonucleotide synthesis was performed on an *ABI-392-08* DNA synthesizer (*Applied Biosystems*, Weiterstadt, Germany) on a 1-μmol scale with the phosphoramidites **9** and **10** and those of the regular 2′-deoxynucleosides (*Applied Biosystems*, Weiterstadt, Germany) according to the synthesis protocol for 3′-phosphoramidites [31]. The crude oligonucleotides were purified and detritylated on oligonucleotide purification cartridges by the standard protocol for purification [26]. The oligonucleotides were lyophilized on a *Speed-Vac* evaporator to yield colorless solids which were stored frozen at −18°. The enzymatic hydrolysis of the oligomers was performed as described in [32]. Quantification of the constituents was made on the basis of the peak areas, which were divided by the extinction

coefficients of the nucleoside (ε_{260} values: A_d 15400, C_d 7300, G_d 11400, T_d 8800, **2a** 6600, **2b** 7300). Snake-venom phophodiesterase (EC 3.1.15.1., *Crotallus durissus*) and alkaline phosphatase (EC 3.1.3.1., *E. coli*) were generous gifts of the *Roche Diagnostics GmbH* (Penzberg, Germany). MALDI-TOF-MS were provided by Dr. *J. Gross* (Universität Heidelberg, Germany). Some selected MALDI-TOF data of modified oligonucleotides are shown in *Table 10*.

Oligonucleotide analysis was carried out by reversed-phase HPLC with a *Merck-Hitachi* HPLC: 250 × 4 mm *RP-18* column; gradients of 0.1M (Et_3NH)OAc (pH 7.0)/MeCN 95:5 (*A*) and MeCN (*B*); gradient I: 50 min 0–50% *B* in *A*, flow rate 1 ml/min; gradient II: 20 min 0–25% *B* in *A*, flow rate 0.7 ml/min, then 30 min 25–40% *B* in *A*, flow rate 1 ml/min; gradient III: 20 min 0–25% *B* in *A*, flow rate 1 ml/min.

Determination of T_m values and Thermodynamic Data. Absorbance *vs.* temp. profiles were measured on a *Cary-1/1E* UV/VIS spectrophotometer (*Varian*, Australia) equipped with a *Cary* thermoelectric controller. The T_m values were measured in the reference cell with a *Pt-100* resistor and the thermodynamic data (ΔH^0, ΔS^0, ΔG^0_{298}) were calculated by means of the 'MeltWin 3.0' program package [27]. CD Spectra: *Jasco-600* (*Jasco*, Japan) spectropolarimeter with a thermostatically (*Lauda RCS-6* bath, Germany) controlled 1-cm cuvette.

We thank Mr. *Yang He* for the NMR spectra, Dr. *Helmut Rosemeyer* for the PSEUROT calculations, and Mrs. *Elisabeth Feiling* for the oligonucleotide syntheses. Financial Support by the *Deutsche Forschungsgemeinschaft* and the *Roche Diagnotics GmbH*, Penzberg, Germany, is gratefully acknowledged.

REFERENCES

[1] W. Saenger, 'Principles of Nucleic Acid Structure', in 'Springer Advanced Texts in Chemistry', Ed. C. R. Cantor, Springer Verlag, New York-Berlin-Heidelberg-Tokyo, 1984.
[2] C. R. Cantor, P. R. Schimmel, 'Biophysical Chemistry', W. H. Freeman & Co., San Francisco, CA, 1980.
[3] E. Uhlmann, A. Peyman, G. Breipohl, D. W. Will, *Angew. Chem., Int. Ed.* **1998**, *37*, 2796, and refs. cit. therein.
[4] K. Groebke, J. Hunzicker, W. Fraser, L. Peng, U. Diederichsen, K. Zimmermann, A. Holzner, C. Leumann, A. Eschenmoser, *Helv. Chim. Acta* **1998**, *81*, 375.
[5] M. Bolli, H. U. Trafelet, C. Leumann, *Nucleic Acids Res.* **1996**, *24*, 4660.
[6] F. Seela, H. Thomas, *Helv. Chim. Acta* **1995**, *78*, 94.
[7] F. Seela, B. Gabler, *Helv. Chim. Acta* **1994**, *77*, 622.
[8] F. Seela, H. Winter, *Helv. Chim. Acta* **1994**, *77*, 597.
[9] F. Seela, P. Leonard, *Helv. Chim. Acta* **1998**, *81*, 2244.
[10] F. Seela, K. Kaiser, *Helv. Chim. Acta* **1988**, *71*, 1813.
[11] F. Seela, H. Steker, *Helv. Chim. Acta* **1985**, *68*, 563.
[12] F. Seela, M. Zulauf, *J. Chem. Soc., Perkin Trans. 1* **1998**, 3233.
[13] F. Seela, M. Zulauf, G. Becher, *Nucleosides Nucleotides* **1997**, *16*, 305.
[14] F. Jordan, H. Niv, *Nucleic Acids Res.* **1977**, *4*, 697.
[15] H. Steker, Dissertation, Universität Paderborn, 1998.
[16] O. Röder, H.-D. Lüdemann, E. von Goldhammer, *Eur. J. Biochem.* **1975**, *53*, 517.
[17] J. Plavec, W. Tong, J. Chattopadhyaya, *J. Am. Chem. Soc*. **1993**, *115*, 9734.
[18] C. A. G. Haasnoot, F. A. A. M. de Leeuw, C. Altona, *Tetrahedron* **1980**, *36*, 2783.
[19] J. van Wijk, C. Altona, 'PSEUROT 6.2, a Program for the Conformational Analysis of Five-Membered Rings', University of Leiden, July, 1993 (licensee: C. Altona, Gorlaeus Laboratories, Leiden, The Netherlands).
[20] H. Rosemeyer, M. Zulauf, N. Ramzaeva, G. Becher, E. Feiling, K. Mühlegger, I. Münster, A. Lohmann, F. Seela, *Nucleosides Nucleotides* **1997**, *16*, 821.
[21] H. Rosemeyer, F. Seela, *J. Chem. Soc., Perkin Trans. 2* **1997**, 2341.
[22] F. Seela, I. Münster, U. Löchner, H. Rosemeyer, *Helv. Chim. Acta* **1998**, *81*, 1139.
[23] F. Seela, G. Becher, H. Rosemeyer, H. Reuter, G. Kastner, I. A. Mikhailopulo, *Helv. Chim. Acta* **1999**, *82*, 105.
[24] F. Seela, H. Debelak, in preparation.
[25] F. Seela, A. Kehne, *Biochemistry* **1985**, *24*, 7556.
[26] Applied Biosystems, 'Manual for Oligonucleotide Purification Cartridges'.
[27] J. A. McDowell, D. H. Turner, *Biochemistry* **1996**, *35*, 14077.

[28] F. Seela, M. Zulauf, *J. Chem. Soc., Perkin Trans. 1* **1999**, 479.
[29] F. Seela, C. Wei, *Helv. Chim. Acta* **1999**, *82*, 726.
[30] G. M. Blackburn, M. J. Gait, in 'Nucleic Acids in Chemistry and Biology', IRL press, Oxford, Vol. 1, p. 33.
[31] Applied Biosystems, 'Users Manual of the DNA synthesizer', p. 392.
[32] F. Seela, S. Lampe, *Helv. Chim. Acta* **1991**, *74*, 1790.

Received April 25, 2000